The challenges of tau imaging

Victor L Villemagne*[1,2], Shozo Furumoto[3], Michelle Fodero-Tavoletti[4], Ryuichi Harada[3], Rachel S Mulligan[1], Yukitsuka Kudo[5], Colin L Masters[2], Kazuhiko Yanai[3], Christopher C Rowe[1] & Nobuyuki Okamura[3]

[1]Department of Nuclear Medicine & Centre for PET, Austin Health, 145 Studley Rd, Heidelberg, VIC 3084, Melbourne, Australia
[2]The Mental Health Research Institute, Melbourne, Australia
[3]Department of Pharmacology, Tohoku University School of Medicine, Sendai, Japan
[4]Department of Pathology, Bio21 Institute, University of Melbourne, Australia
[5]Innovation of New Biomedical Engineering, Center Tohoku University, Sendai, Japan
*Author for correspondence: Tel.: +61 3 9496 5321, Fax: +61 3 9458 5669, victorv@unimelb.edu.au

In vivo imaging of tau pathology will provide new insights into tau deposition in the human brain, thus facilitating research into causes, diagnosis and treatment of major dementias, such as Alzheimer's disease, or some variants of frontotemporal lobar degeneration, in which tau plays a role. Tau imaging poses several challenges, some related to the singularities of tau aggregation, and others related to radiotracer design. Several groups around the world are working on the development of imaging agents that will allow the *in vivo* assessment of tau deposition in aging and in neurodegeneration. Development of a tau imaging tracer will enable researchers to noninvasively examine the degree and extent of tau pathology in the brain, quantify changes in tau deposition over time, evaluate its relation to cognition and assess the efficacy of anti-tau therapy.

Alzheimer's disease (AD), the leading cause of dementia in the elderly, is an irreversible, progressive neurodegenerative disorder clinically characterized by memory loss and cognitive decline [1], leading invariably to death, usually within 7–10 years after diagnosis. AD accounts for 50–70% of dementia cases [2], followed by frontotemporal lobar degeneration (FTLD), which is responsible for 10–20% of cases [3,4]. At present, patients exhibiting signs of dementia are diagnosed based on clinical and neuropsychological examination; however, FTLD is a syndrome that can be clinically difficult to distinguish from AD, especially in the early stages of the disease. Still today, definitive diagnosis of these neurodegenerative conditions can only be established after post-mortem examination of the human brain.

Genetic, pathological, biochemical and cellular evidence implicating the amyloid precursor protein and its proteolytic product β-amyloid (Aβ) as being central to AD etiology still remains contentious [5]. Human postmortem studies have shown that while soluble Aβ oligomers and the density of neurofibrillary tangles (NFTs) strongly correlate with neurodegeneration and cognitive deficits, the density of Aβ insoluble plaques does not [6–11], and Aβ burden, as assessed by PET, does not strongly correlate with cognitive impairment in AD patients [12,13]. Cortical NFTs are not observed in cognitively unimpaired individuals, in contrast to Aβ plaques, which appear abundantly in some nondemented people [12,14–16]; higher brain Aβ burden is typically seen in hereditary forms of cerebral amyloid angiopathy, without accompanying NFT formation. The lack of a strong association between Aβ deposition and measures of cognition, synaptic activity and neurodegeneration in AD, in addition to the evidence of Aβ deposition in a high percentage of asymptomatic healthy controls, suggests that Aβ is an early and necessary, although not sufficient, cause for cognitive decline in AD [17]. This points to the involvement of other downstream mechanisms, such as NFT formation, leading to synaptic failure and eventually neuronal loss.

The physiological function of tau is to bind to tubulin to stabilize microtubules, which is critical for the axonal support of neurons. Based on the number of tubulin-binding repeats within the protein, six tau isoforms have been identified [18]. While the underlying mechanisms leading to tau hyperphosphorylation, misfolding and aggregation remain unclear, tau aggregation and deposition follows a stereotyped spatiotemporal pathway both at the intraneuronal level [19,20] as well as in its topographical and neuroanatomical distribution in the brain [21–25]. Mutations have been identified within the tau gene (*MAPT*) leading to frontotemporal dementia with Parkinsonism linked to chromosome-17 [26], providing solid evidence that tau malfunction triggers neurodegeneration and dementia.

Neurodegenerative diseases characterized by pathological tau accumulation are termed 'tauopathies'. Along with AD and some variants

Keywords

- Alzheimer's disease
- frontotemporal lobar degeneration
- molecular neuroimaging
- neurodegeneration
- radiotracer design
- tau

Future Medicine part of fsg

of FTLD, other tauopathies include Down's syndrome, Guam Parkinsonism–dementia complex, dementia pugilistica, frontotemporal dementia with Parkinsonism linked to chromosome-17, corticobasal degeneration (CBD), progressive supranuclear palsy (PSP) and chronic traumatic encephalopathy [24,27–30]. While these conditions share tau immunoreactivity in post-mortem analysis, they can be composed of different tau isoforms and show distinct histopathological and ultrastructural differences [28,31]. For example, a diversity of tau deposits can be recognized histologically in these diseases, either as NFTs, neuropil or glial threads, Pick bodies, dystrophic neurites in plaques, astrocytic plaques or coiled bodies, among others [24,28].

The notion that tau deregulation could be a key mediator of neurodegeneration [26,32–34] has stimulated the development of therapeutics for the treatment of AD and non-AD tauopathies. Inhibition of abnormal tau hyperphosphorylation, its aggregation or direct stabilization of microtubules, appears to be a promising therapeutic strategy that may cure or retard the development of these diseases [35–43]. Given that these treatments are currently being developed, a noninvasive method of determining both the tau load and its regional cerebral patterns would not only assist in the early and differential diagnosis of AD and non-AD tauopathies, but also facilitate monitoring the efficacy of such new treatments.

Modern molecular imaging procedures may overcome the need for a neuropathological examination of brain tissues by noninvasively identifying the underlying pathology of these diseases, rather than relying solely on clinical symptoms and neuropsychological assessments. In recent years, considerable effort has been focused on imaging agents for the early diagnosis of neurodegenerative diseases such as AD. So far, the main focus has been placed on the development of novel Aβ ligands that are permitting early detection of Aβ deposition [12,44]. Among these tracers, ^{18}F-FDDNP was claimed to not only bind to Aβ deposits but to also bind to NFTs [45]. Furthermore, *in vitro* studies using tracer concentrations similar to those achieved during a PET scan (~1 nM) showed that ^{18}F-FDDNP failed to bind to NFTs and that it binds weakly to Aβ plaques [46]. Therefore, the development of a selective and specific imaging agent for tau imaging is critical for developing a more profound understanding of the pathophysiology of AD, FTLD and other neurodegenerative conditions, but will also lead to improvements in differential diagnostic accuracy and also accelerate treatment discovery and monitoring of therapeutics.

Tau imaging poses several challenges, some related to tau aggregation and deposition and others related to radiotracer design (Box 1).

Challenges related to tau as an imaging target

Tau is a phosphoprotein and the degree of phosphorylation determines its binding abilities to microtubules. tau hyperphosphorylation leads to weaker microtubule binding and an increase of unbound phospho-tau concentration in the cytosol [47]. This accumulation leads to the formation of filaments that form the pathologic tau aggregates in the form of filamentous inclusions, [48] found in neurons, astrocytes and oligodendroglia [49].

Intracellular location

Tau aggregates are mainly intracellular although, to a much lesser degree, they are also found extracellularly when, as neurons die, the intracellular tau deposits become extracellular (i.e., 'ghost tangles' found in AD). The intracellular location of tau aggregates means that a neuroimaging radiotracer not only has to be able to cross the blood–brain barrier (BBB) but also has to cross the cell membrane, either by active transport or passive diffusion, to reach its target. This posits an extra set of constraints in tracer design in terms of lipophilicity as well as molecular size. There are several examples showing that the challenge of imaging intracellular targets is achievable just as illustrated by the imaging of vesicular transporters either for acetylcholine [50] or monoamines [51,52] or imaging the aromatase responsible for converting androgens into estrogens [53,54].

Six isoforms leading to different phenotypes

Not all tau aggregates are the same. In the human brain, alternative mRNA splicing of a single gene transcript generates six tau isoforms, and their presence or absence lead to different phenotypes [55,56]. These isoforms differ in whether they contain exon 2, exon 3 and exon 10, manifested in the presence or absence of the fourth microtubule-binding domain (coded for in exon 10) and the presence or absence of one (exon 2) or two (exons 2 and 3) N-terminal inserts (Figure 1) [57]. Based on the number of microtubule binding domains these tau isoforms have been classified into two functionally different groups: those with three microtubule binding domains, called three repeat tau (3R), and those with four microtubule binding domains, called four repeat

tau (4R) [58]. Normally there is an equal ratio of three repeat tau/four repeat tau, and it has been proposed that changes to this ratio might lead to neurodegeneration [59]. Based on the isoform, these abnormal intracellular tau inclusions adopt different morphologies [31,60]. For example, when examined under the light microscope, tau inclusions are found as NFTs in AD, (Figure 1B) [31,61] astrocytic plaques in CBD [62] or Pick's bodies in Pick's disease (Table 1) [63]. Ultrastructurally, these aggregates are either paired helical (PHF), straight (SF), or randomly coiled filaments (RCF) (Table 1) [28,31,64] . Polymorphism is the rule, with the same tau isoform adopting multiple conformations, and different isoforms adopting similar ultrastructural forms (Figure 1C) [65] . PHF is the predominant form found in NFTs, and despite certain controversy, *in vitro* experiments with PHFs suggest a β-sheet-structured core similar to the characteristic β-sheet structure adopted by Aβ and α-synuclein fibrillar aggregates [66,67]. The brain distribution of these tau aggregates is different in the different phenotypes. While this might be an advantage for the differential diagnosis of tauopathies, it assumes that the same tau ligand binds equally to the whole spectrum of tau polymorphism; however, this is unlikely.

Multiple variants of post-translational modifications

To make matters worse, there are several post-translational modifications that might change the conformation of the aggregates. The most common of these modifications is phosphorylation that leads to dissociation from the microtubules followed by aggregation. But there are several other post-translational modifications, such as acetylation, glycosylation, glycation, prolyl-isomerization, nitration and ubiquitination (for review see [68]), which might affect the conformation of the aggregates and thus the ability of specific tracers to bind to tau. This has been extensively shown to be the case with Aβ aggregates where conformational changes have an effect on tracer binding. For example, nonhuman primates produce and accumulate Aβ with an identical amino acid sequence to human Aβ but they neither present the full phenotype of AD nor do they show Pittsburgh Compound B (PiB) binding despite the presence of plaques [69,70]. Understanding the polymorphism of these tau aggregates might help develop more specific imaging agents.

Tau aggregates in white matter

Not only are there typical tau aggregates in predominantly white matter regions as observed in the brainstem of PSP and CBD patients [62,71], but substantial abnormal tau aggregate levels have also been shown in subcortical white matter in AD [72–74], Pick's disease [75], or even in some cases of sporadic FTLD [76]. In contrast to Aβ imaging, in which white matter binding has been shown to be nonspecific [77], these reports highlight the fact that some degree of specific white matter binding by tau imaging compounds should be expected. Additionally, given the ~50% lower regional cerebral blood flow in white matter compared with the neocortex [78,79], it might not be an easy task to discriminate between specific and nonspecific binding.

Box 1. Characteristics of tau tracer.

I. Characteristics of tau deposits

- Intracellular
- Six isoforms leading to different phenotypes
- Multiple variants of post-translational modifications
- Tau aggregates in white matter
- In Alzheimer's disease, tau aggregates are coexistent with β-amyloid deposits
- In Alzheimer's disease, there are lower concentrations of tau than β-amyloid

II. Characteristics of tau radiotracer

- Easily labeled with isotopes with long decay half-lives
- High binding potential
- High selectivity for tau over β-amyloid
- High blood–brain barrier permeability
- Low nonspecific binding
- No or low metabolism

In AD, tau aggregates are coexistent with Aβ deposits

Another issue to be considered is the coexistence of other misfolded proteins sharing the same β-sheet secondary structure, as in the case of AD where tau and Aβ are both colocalized in gray matter structures. This issue goes to the core of binding selectivity, affecting tracer design strategies. Aβ imaging agents, such as PiB, show a distinct selectivity for fibrillar Aβ deposits [80] over tau [81,82] and α-synuclein [83,84]. A similar binding profile, with high selectivity for tau over Aβ and α-synuclein is paramount for a successful tau imaging agent.

In AD, there are lower concentrations of tau than Aβ

In AD, the issue of selectivity is further complicated by the disparity between the brain concentrations of tau and Aβ aggregates, where the

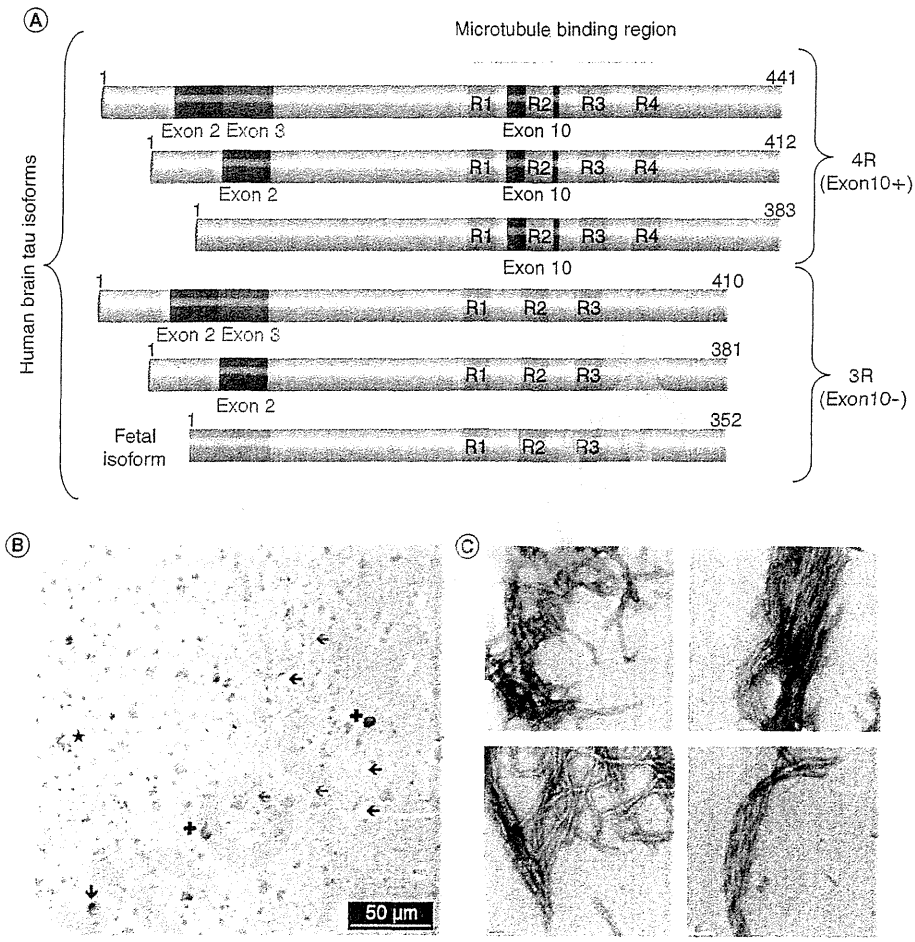

Figure 1. TITLE. (A) Schematic representation of the six different tau isoforms found in the human brain. Isoforms are characterized by the presence or absence of exon 10 resulting in either 3 (3R) or 4 (4R) repeats of the microtubule binding domain. Different combinations of these isoforms manifest as different phenotypes. For example PSP and CBD are characterized by presenting 4R tau, while Pick's disease is a 3R tauopathy. In AD, both 3R and 4R are present. **(B)** Immunohistochemical analysis depicting pathological tau deposits in the hippocampus of an Alzheimer's disease patient: microscopy images show numerous neurofibrillary tangles (✚), dystrophic neurites (★), numerous neuropil threads (←), and a ghost tangles (↓). Sections are immunostained with tau polyclonal antibody (DAKO). **(B)** Scale bar = 50 µm. **(C)** Variable tau fibril morphology evidenced by electron microscopy. Electron micrographs of recombinant tau constructs showing tau fibrillar polymorphism. Recombinant tau construct K18ΔK280 (top) comprising the four repeats in the microtubullar domain with deletion at K280 and recombinant tau construct K19Y310W (bottom) comprising three repeats in the microtubullar domain with the tyrosine 301 mutated into tryptophan. **(C)** Scale bars = 50 nm. CBD: Corticobasal degeneration; PSP: Progressive supranuclear palsy.
(A) Adapted from [18,55].

concentrations of tau aggregates are ~5–20-times lower than those of Aβ. As in any other PET technique, tau imaging is predicated on measuring the concentration of bound tracer within a brain region. Based on the results by Naslund and colleagues [85], the $A\beta_{1-40}$ and $A\beta_{1-42}$ brain concentrations in AD range between 400–1900 pmol/g wet tissue, while the reported concentrations for PHF-tau in the same areas range between 50 and 200 pmol/g wet tissue (Figure 2) [73]. Despite this imbalance, there is a distinct regional pattern of Aβ and tau distribution in the neocortex. While the highest concentrations of Aβ deposits are found in the frontal cortex, the highest concentrations of PHF-tau are found in the temporoparietal cortices (Figure 3) [73,85].

Table 1. Pathological and ultrastructural correlations of tau isoforms in different types of tauopathies.

Type	Pathology	Tau isoform	Light microscope	Electron microscope
I	Alzheimer's disease	3R and 4R	Neurofibrillary tangles	PHF and SF
	Down's syndrome	3R and 4R	Neurofibrillary tangles	PHF and SF
II	Corticobasal degeneration	4R	Astrocytic plaques	SF and TF
	Progressive supranuclear palsy	4R	Globose tangles; Tufted astrocytes	SF and TF
III	Pick's disease	3R	Pick's bodies	RCF and SF
IV	Myotonic dystrophy	Short 3R	Neurofibrillary tangles	N/A

N/A: Not available; PHF: Paired helical filaments; RCF: Random coil filaments; SF: Straight filaments; TF: Twisted filaments. Adapted from [64].

Another issue that might be raised is in regard to the actual concentration of tau aggregates and whether this concentration is sufficient to allow imaging. As detailed above, the tau concentrations in gray matter are at least an order of magnitude higher than the concentration of many receptors successfully assessed by PET [86,87].

Challenges related to radiotracer design

For a radiotracer to be useful as a neuroimaging probe, a number of key general properties are desirable: they should be nontoxic lipophilic molecules of low molecular weight (<450) that cross the BBB, with rapid clearance from blood and preferably not metabolized, whilst reversibly binding to its target in a specific and selective fashion [88–91]. Overall, binding affinity and lipophilicity are the most crucial properties for *in vivo* radioligands. Furthermore, low nonspecific binding is desirable (Box 1).

Easily labeled with isotopes with long decay half-lives

The 20-min radioactive decay half-life of carbon-11 (^{11}C) limits the use of ^{11}C tracers to centers with an on-site cyclotron and ^{11}C radiochemistry expertise, making the access to these tracers restricted and with costs prohibitive for routine clinical applications [92]. To overcome these limitations, tau tracers should ideally be labeled with isotopes with longer half-lives, such as fluorine-18 (^{18}F; half-life of ~2 h) or copper-64 (^{64}Cu; half-life of ~13 h) for PET, or technetium-99m (half-life of ~6 h) or iodine-123 (^{123}I; half-life of ~13 h) for single photon emission computed tomography, which allows centralized production and regional distribution, as currently practiced worldwide in the supply of ^{18}FDG or technetium-99m generators/radiopharmaceuticals for clinical use [93–95].

High binding potential

Usually, the overall binding of a tracer can be predicted by the ratio of the total number of available binding sites (B_{max}) over the affinity (K_D) for the target. At steady state, this ratio is denominated the binding potential (BP) [96]. In the case of AD where the target protein (tau) is surrounded by another more abundant protein (Aβ), which shares a similar secondary β-sheet structure, the BP for PHF-tau should be higher than for Aβ. This can either be achieved by a tracer that binds to more sites (higher B_{max}) or, most likely, a tracer with higher affinity for

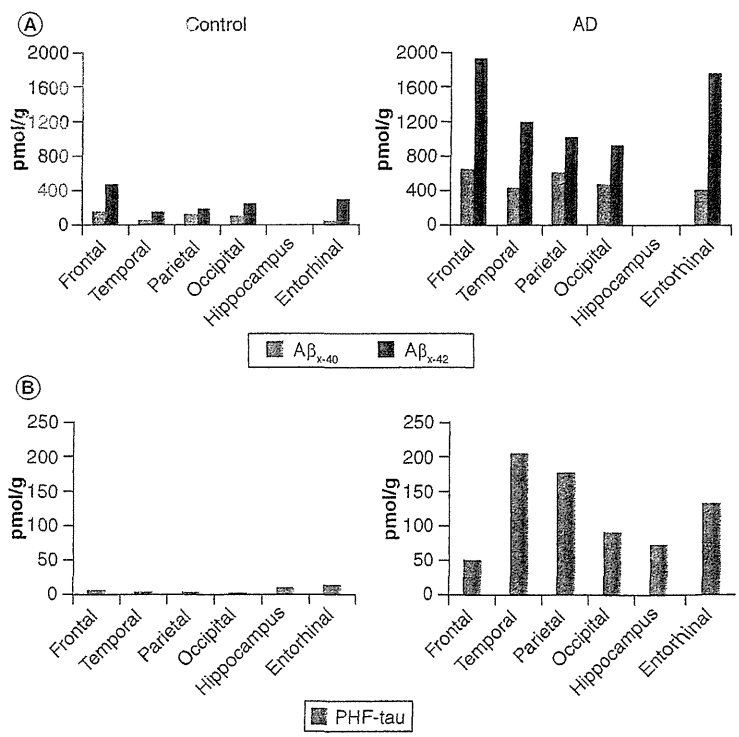

Figure 2. Regional brain concentrations of $A\beta_{x-40}$, $A\beta_{x-42}$, and paired helical filament–tau in Alzheimer's disease. β-amyloid concentrations are substantially higher than PFH-tau. While Aβ concentrations are higher in the frontal cortex than in temporal or parietal cortices, PHF-tau concentrations in temporal or parietal cortices are higher than in frontal cortex.
PHF: Paired helical filament.
Data taken from [73,85].

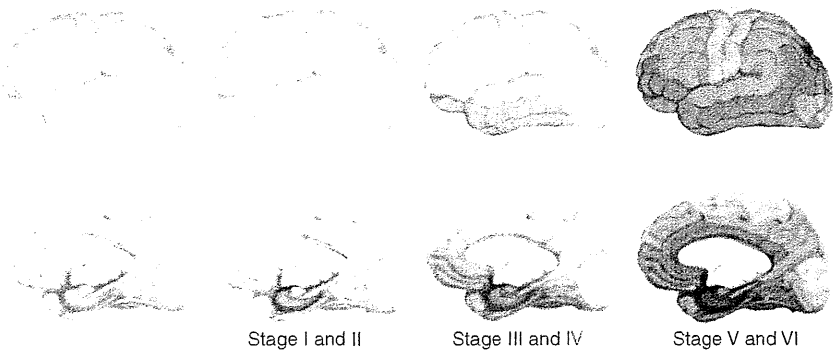

Figure 3. Different stages of tau deposition in Alzheimer's disease. Earliest area of tau deposition is usually found in the enthorinal cortex and hippocampal formation. Cognitive impairment becomes apparent when tau deposition involves cortical polymodal associations areas (Braak Stages IV–VI).
Adapted from [21,25].

PHF-tau (lower K_D). While selective tau tracers with higher *in vitro* BP for PHF-tau than for Aβ have already been described [97,98], their higher BP might not be enough to overcome the higher Aβ concentrations *in vivo*. Lipophilicity is one of the major determinants of binding affinity and tracer kinetics, where higher affinities are usually associated with slower kinetics and therefore, longer scanning times. While radioligands with lower binding affinity normally display faster *in vivo* brain kinetics, at the same time they exhibit insufficient specific binding. Therefore, finding the optimal lipophilicity is a keystone in the design of tau radioligands.

High selectivity for tau over Aβ

The selectivity required for a particular neuroimaging radiotracer depends on the concentration of available binding sites [89]. As mentioned before, in AD there are higher cortical concentrations of Aβ compared with PHF-tau. Therefore, exquisite selectivity is required for a tau radioligand. One way of testing this is, as already described, is by designing ligands with a high *in vitro* tau–BP/Aβ–BP ratio. Another way to ascertain high selectivity is through *in vitro* autoradiography (ARG) studies of AD brain sections, where both Aβ and PHF-tau are present. The advantage of ARG is that it can be performed at very low concentrations of the tracer (~1 nM), similar to those achieved during a PET scan, and simultaneously in several brain regions or different neurodegenerative conditions allowing the screening of different compounds against a wide spectrum of targets [99]. Whole hemisphere ARG also allows the examination of several regions of the brain with a different Aβ/PHF-tau ratio. *In vitro* as well as *ex vivo* ARG studies also provide some information with regard to signal-to-noise ratio of the specific signal by allowing the examination of the nonspecific binding in the surrounding tissues [100]. While *in vitro* reports have already shown that based on K_D alone, a 3–12-fold selectivity for PHF-tau is attainable [97,101,102], simulation studies estimate that a 20–50-fold selectivity for PHF-tau over Aβ will be required to image PHF-tau *in vivo* [103].

High BBB permeability

Most successful neuroimaging radiotracers show an initial brain uptake above 5% of the injected dose at 2 min after intravenous injection [90]. This brain uptake depends on several factors such as cerebral regional blood flow, BBB permeability, plasma radiotracer concentration and free fractions of the radiotracer in plasma and in the brain [90]. Lipophilicity is one of the most important physicochemical properties for neuroimaging radiotracers owing to its direct relationship to membrane permeability, solubility in water and entropic contribution to binding [104]. It is well known that lipophilic drugs can readily cross the BBB, although other drug parameters, including the number of hydrogen bonds, molecular weight, polar surface area and molecular 'bulkiness' are liable to passive transport. Lipophilicity is a parameter commonly used in the design of radioligands. It is usually expressed as the log octanol/water coefficients ($LogP_{OCT}$), the partition coefficient for nonionized compounds between octanol and water. Ideally a ligand sufficiently lipophilic to adequately cross the

BBB should exhibit $LogP_{OCT}$ values between 0.9 and 3.0 [105]. Within this optimal range, more lipophilic radioligands will display faster accumulation of radioactivity in the brain than less lipophilic ones. Conversely, compounds that are too lipophilic will be bound by plasma proteins and usually undergo fast metabolism, thus displaying a lower CNS uptake.

Low nonspecific binding

High brain penetration alone is not enough. What is relevant in imaging is the ratio of specific to nonspecific binding [89]. Most importantly, lipophilic radioligands display higher nonspecific binding. Therefore, the less lipophilic of two or more radiotracers with similar physicochemical profiles should exhibit a higher BP. The lowest possible lipophilicity is desirable for minimizing the nonspecific binding of a radioligand [89]. Low lipophilicity is especially important if the values of the specific and nonspecific distribution volumes are comparable [106]. Ligands with a similar K_D may display quite different association (k_{on}) and/or dissociation (k_{off}) rates from the target. While a higher k_{off} reflects faster clearance, a higher association rate corresponds to faster *in vivo* uptake. Commonly, high-affinity neuroimaging ligands are characterized by a low k_{off}, while lower affinity ligands exhibit a higher k_{off} [107]. In order to obtain a good signal-to-background ratio a neuroimaging radiotracer also needs fast clearance from nonspecific areas. A good index of the clearance of the tracer from nonspecific areas can be inferred from the brain 2 min over 30-min or 60-min ratio ratio in wild-type mice or nonhuman primate biodistribution/imaging studies. Most successful neuroimaging radiotracers present with high 2–30-min ratios (>8–10), reflecting a fast clearance from regions that do not contain the target.

No or low metabolism

Ideally, a PET radiotracer should readily enter the brain and selectively bind to its target in the absence of radiolabeled metabolites [90]. Neuroimaging radiotracers are usually immediately exposed to a wide spectrum of metabolizing enzymes in the blood and other tissues as soon as they are injected. Most radiotracers exhibit significant degradation just minutes after injection, and the blood concentration of the unmetabolized fraction of the original radiotracer declines very rapidly. Given that PET has no means to distinguish between the chemical sources of detected radioactivity, the fate of the radioactive isotope is paramount, especially if radiolabeled metabolites cross the BBB and either remain unbound or bind to a different target [90]. In most cases these radiolabeled metabolites are less lipophilic than the original radiotracer and therefore less likely to enter the brain. Defluorination, leading to bone accumulation of ^{18}F, is another issue observed in ^{18}F-labeled radiotracers. A way to reduce potential metabolism and defluorination can sometimes be addressed at the radiotracer design stage (for review see [90]).

Strategies for developing tau imaging tracers

Most of the research efforts are focused on imaging tracers for PHF-tau that is the ultrastructural form that tau aggregates adopt in AD. It is not clear at this stage if or how well these tracers bind to the other conformations of tau aggregates present in non-AD tauopathies. The polymorphism of tau aggregates might be an important aspect to be considered in tracer design. It is important to keep in mind that different conformations of tau deposits in the brain, as is the case with Aβ [69], may affect the binding characteristics of the tracers because they may not recognize all types of tau pathologies with the same degree of sensitivity. The relevance of the conformation of the aggregates is clear in Aβ imaging studies where in some cases of familial autosomal dominant forms of AD [108,109] or early stages of Aβ deposition [110], when the aggregates lack the typical fibrillar Aβ conformation seen in sporadic, late-onset AD, there is little PiB binding. Furthermore, nonhuman primates produce and have Aβ deposits that are identical in amino acid sequence to human Aβ, but none of them exhibit the full AD phenotype, and most importantly, they do not bind PiB even in the presence of plaques [70], and transgenic mice producing human Aβ exhibit considerably less Aβ binding sites in the mouse brain than in the human AD brain [44]. This illustrates the importance of polymorphism in regards to ligand binding.

After the success of Aβ imaging with PiB [111], there is a renewed international effort to develop selective tau ligands. Most research groups proposing PHF-tau imaging tracers are groups working on therapeutic tau anti-aggregation or defibrillization strategies [101,112,113,201], while some others are focused on screening novel or available chemical libraries in order to identify high-affinity selective PHF-tau compounds amenable to radiolabeling [202–204].

One group based in Hamburg, Germany is exploring differential binding selectivity

for tau and $A\beta_{1-42}$ fibrils based on the structure activity relationship of *N'*-benzylidene-benzohydrazides. Assessment of target selectivity is based on the anti-aggregating activity and fluorescent staining profile achieved with amphiphilic compounds. Based on these results, a strategy for target selectivity was proposed, where selectivity towards PHF-tau is achieved by incorporating into these amphiphilic ligands bulky hydrophilic groups not tolerated by Aβ fibrils. Thus, some compounds (e.g., BSc4000) exhibited selective PHF-tau staining, while others (e.g., BSc3994) presented with selective Aβ plaque staining [112]. Efforts to customize and radiolabel these derivatives to make them viable for PHF-tau imaging with PET are ongoing.

Focused on PHF-tau therapeutics [42,114], a group based in Aberdeen, Scotland, also assessed benzothiazole, imidazothiazole and pyrimidazole derivatives in displacement studies with primuline and in fluorescent studies in human and tau transgenic mouse brains [201]. One of these compounds, SKT04–137, was radiolabeled with ^{18}F for biodistribution studies in mice, where it showed sufficient brain uptake but slow clearance from the brain (2 min over 60-min ratio) [201].

One group from Ohio (USA), is proposing to achieve PHF-tau selectivity through structure activity relationship and tracer docking simulation studies with 2-aryl benzothiazole derivatives showing distinct binding profiles by altering the side chain composition of the compounds, as a way of addressing differences in protein composition and structural polymorphism [101,115].

A team of researchers from Santiago, Chile, proposed the use of the benzimidazole derivatives astemizole and lansoprazole as potential PHF-tau imaging agents based on their ability to bind Aβ *in vitro* and recombinant tau fibrils, as well as PHF-tau isolated from AD brains. While astemizole K_D was similar for PHF-tau and Aβ, the respective B_{max} were different yielding higher BP for PHF-tau than for Aβ (3.0 vs 0.06, respectively). While no 2-min data is available in the reported pharmacokinetic studies, both compounds seem to show very slow uptake and clearance profiles [98].

Using *in vitro* autoradiography, a group from Siemens (California, USA), has identified several novel benzimidazole pyrimidines that bind to human PHF-tau. Two of the best candidates, ^{18}F-T777 and ^{18}F-T808, with a K_D of 19 and 22 nM, respectively, show >25-fold selectivity for PHF-tau over Aβ [203].

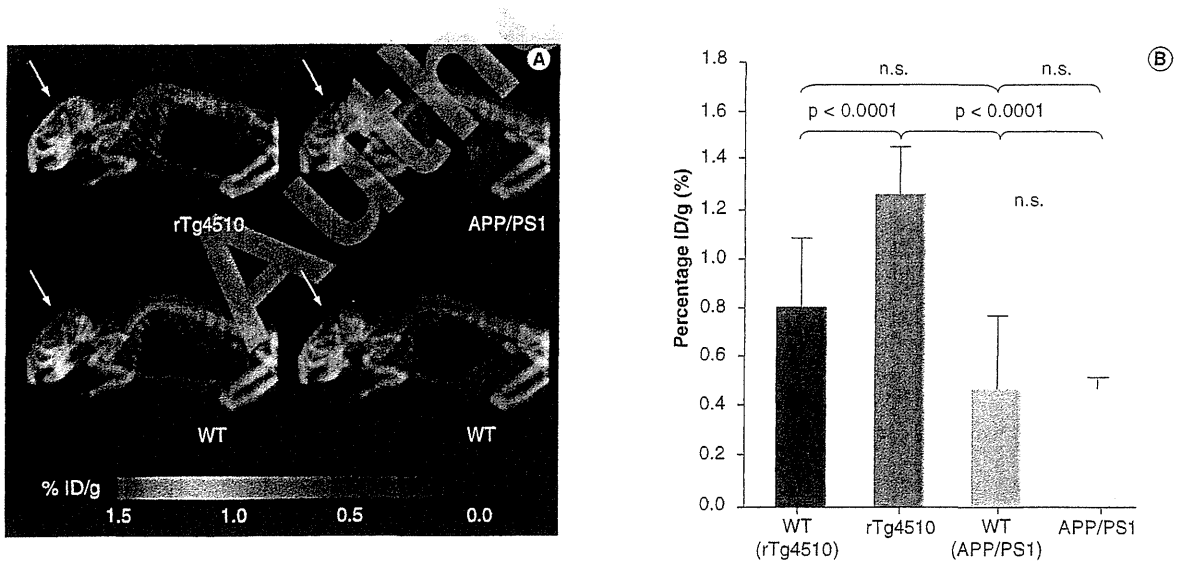

Figure 4. Preclinical evaluation of 18F-THK523 a novel tau imaging radiotracer. (A) Representative 18F-THK523 fusion microPET/CT images of tau and Aβ transgenic mice at 30-min postinjection. rTg4510 mice (top, left) exhibited higher 18F-THK523 brain retention compared to their wild-type (WT) littermate (bottom, left). Low 18F-THK523 retention was observed in APP/PS1 (top, right) versus their wild-type littermates (bottom, right). **(B)** Bar graphs showing 18F-THK523 microPET retention in the brain of rTg4510, APP/PS1 and their respective wild-type mice at 30 min postinjection. Brain 18F-THK523 retention was significantly higher in rTg4510 mice compared to APP/PS1 mice and their respective wildtype littermates.
Adapted from Fodero-Tavoletti *et al.* [97].

Since 2002, the Tohoku University group in Japan has been designing and screening benzoxazole, benzimidazole, quinoline and other derivatives targeting β-sheet structures in brain sections [102,116,202,204]. Recently published results on one of these derivatives, ^{18}F-THK523 is probably the most advanced PHF-tau imaging agent reported in the literature to date, with a 20-fold higher BP for PHF-tau compared with $A\beta_{1-42}$ [97]. Further evidence of ^{18}F-THK523 PHF-tau selectivity was demonstrated by autoradiography and in fluorescence studies where even at concentrations 10,000-fold higher than those typically achieved under PET studies, THK523 failed to highlight Aβ plaques, colocalizing with tau pathology in human AD hippocampal sections. MicroPET studies showed significant higher retention in rTg4510 tau transgenic mice brains compared with Aβ (APP/PS1) transgenic mice or their corresponding wild-type littermates (FIGURE 4) [97].

Conclusion

There are several challenges on the horizon for tau imaging. In AD, a tau radiotracer needs to be highly selective to overcome higher Aβ concentrations. Different conformations, either due to specific tau isoforms or different post-translational modifications, might mean that a radiotracer that is able to identify PHF-tau might not be able to bind other known tau ultrastructural conformations.

There are also challenges in the design of a tau imaging radiotracer. The candidate tau radiotracer should be amenable for high specific activity labeling with ^{18}F or other long-lived radioisotopes to allow a wider and more cost-effective application of the technique. It should be a lipophilic, nontoxic small molecule with a high specificity and selectivity for tau, with no radiolabeled metabolites that enter the brain. The current research indicates that the design of tau radioligands with subnanomolar affinity for tau with an appropriate lipophilicity might be feasible. While a high affinity for tau is desirable to provide an adequate signal-to-noise ratio, it might also delay reaching binding equilibrium requiring extending the scanning time. While lipophilicity is necessary for the tracer to cross the BBB, if the radiotracer is too lipophilic, its nonspecific binding might be too high [89,90].

Future perspective

In vivo imaging of tau pathology by PET will allow new insights into tau deposition in the human brain, facilitating research into causes, diagnosis and treatment of major dementias, such as AD or some variants of FTLD, in which tau plays a role. The development of a specific tau imaging technique will allow the assessment of the regional tau burden in the brain of AD patients, thus providing a link between brain Aβ pathology and neurodegeneration [97,117,118]. It will aid in the gathering of crucial information on the neurobiology of AD and non-AD tauopathies, by allowing the time course of tau accumulation to be correlated with current and future cognitive function. In conjunction with amyloid imaging, it may improve the specificity of diagnosis and allow for early detection of AD pathology in at-risk individuals.

Therapies, especially those targeting irreversible neurodegenerative processes have a better chance of succeeding if applied early. That is why early detection of the underlying pathological process is so important. Therapeutic trials aimed at modulating PHF-tau have been conducted or are currently underway [114,119,120]. Tau imaging will allow noninvasive clinical evaluation and selection of those individuals most likely to benefit from disease-modifying therapy. Furthermore, in order to properly correlate whether the efficacy of these treatments is truly associated with modifying PHF-tau deposition, it will be necessary to quantify tau burden in living patients.

The growing body of research focused on the development of radiotracers for tau imaging is allowing researchers to distinguish specific radiotracer characteristics that are relevant for selective and specific binding to tau aggregates. There is still plenty of room for improvement. Development of new ligands and new leads are crucial for further progress in this promising field.

Acknowledgements

The authors would like to thank Roberto Cappai and Kevin J Barnham for fruitful discussions.

Financial & competing interests disclosure

This study was supported in part by research grant from the Alzheimer's Drug Discovery Foundation (20101208 AFTD) and by a grant from the Industrial Technology Research Program of the New Energy and Industrial Technology Development Organization (NEDO) of Japan. The authors have no other relevant affiliations or financial involvement with any organization or entity with a financial interest in or financial conflict with the subject matter or materials discussed in the manuscript apart from those disclosed.

No writing assistance was utilized in the production of this manuscript.

Challenges related to tau as an imaging target

- Intracellular tau aggregates are constituted by different isoforms and undergo multiple post-translational modifications leading to heterogenous ultrastructural conformations. Not only are they found in gray matter areas, but they are also present, albeit to a lesser degree, in white matter. In Alzheimer's disease (AD), tau aggregates are present in much lower concentrations than those of coexistent Aβ.

Challenges related to radiotracer design

- Successful neuroimaging radiotracers need to be nontoxic lipophilic molecules of low molecular weight that cross the blood–brain barrier, are rapidly cleared from blood and are preferably not metabolized. On top of the described general characteristics for a neuroimaging radiotracer, tau imaging radiotracers must be extremely selective to be able to bind exclusively to tau aggregates and, as is the case in AD, demonstrate no binding to coexistent Aβ.

Strategies for developing tau imaging tracers

- The heterogenous ultrastructural conformations of tau aggregates pose a challenge for radiotracer design. There are several groups working on developing selective tau radiotracers. Because paired helical filaments–tau is the predominant ultrastructural conformation found in AD, and AD is the most prevalent of tauopathies, most of the effort is focused on developing PHF-tau imaging tracers.

Conclusion

- There are several challenges for tau imaging. In AD, a tau radiotracer needs to be highly selective to overcome higher Aβ concentrations. Different conformations of the tau aggregates suggest that a radiotracer that is able to identify PHF-tau might not be able to bind other known tau ultrastructural conformations.

Future perspective

- *In vivo* imaging of tau pathology by PET will allow new insights into tau deposition in the human brain, facilitating research into causes, diagnosis and treatment of major neurodegenerative conditions in which tau plays a role. It will aid in the gathering of crucial information regarding tau deposition in tauopathies, allowing longitudinal assessment of tau accumulation and its relation to cognition. Tau imaging will also allow better selection of candidates for therapeutic trials, as well as assessment of the efficacy of anti-tau therapy.

References

Papers of special note have been highlighted as:
- ▪ of interest
- ▪▪ of considerable interest

1. Khachaturian ZS. Diagnosis of Alzheimer's disease. *Arch. Neurol.* 42(11), 1097–1105 (1985).
2. Masters CL, Cappai R, Barnham KJ, Villemagne VL. Molecular mechanisms for Alzheimer's disease: implications for neuroimaging and therapeutics. *J. Neurochem.* 97(6), 1700–1725 (2006).
3. Neary D, Snowden JS, Gustafson L *et al.* Frontotemporal lobar degeneration: a consensus on clinical diagnostic criteria. *Neurology* 51(6), 1546–1554 (1998).
4. Ratnavalli E, Brayne C, Dawson K, Hodges JR. The prevalence of frontotemporal dementia. *Neurology* 58(11), 1615–1621 (2002).
5. Hardy J. Amyloid, the presenilins and Alzheimer's disease. *Trends Neurosci.* 20(4), 154–159 (1997).
6. Duyckaerts C, Brion JP, Hauw JJ, Flament-Durand J. Quantitative assessment of the density of neurofibrillary tangles and senile plaques in senile dementia of the Alzheimer type. Comparison of immunocytochemistry with a specific antibody and Bodian's protargol method. *Acta Neuropathol.* 73(2), 167–170 (1987).
7. Duyckaerts C, Delaere P, Hauw JJ *et al.* Rating of the lesions in senile dementia of the Alzheimer type: concordance between laboratories. A European multicenter study under the auspices of EURAGE. *J. Neurol. Sci.* 97(2–3), 295–323 (1990).
8. Delaere P, Duyckaerts C, Brion JP, Poulain V, Hauw JJ. Tau, paired helical filaments and amyloid in the neocortex: a morphometric study of 15 cases with graded intellectual status in aging and senile dementia of Alzheimer type. *Acta Neuropathol.* 77(6), 645–653 (1989).
9. Arriagada PV, Growdon JH, Hedley-Whyte ET, Hyman BT. Neurofibrillary tangles but not senile plaques parallel duration and severity of Alzheimer's disease. *Neurology* 42(3 Pt 1), 631–639 (1992).
10. Dickson DW. Neuropathological diagnosis of Alzheimer's disease: a perspective from longitudinal clinicopathological studies. *Neurobiol. Aging* 18(Suppl. 4). S21–S26 (1997).
11. Mclean CA, Cherny RA, Fraser FW *et al.* Soluble pool of Aβ amyloid as a determinant of severity of neurodegeneration in Alzheimer's disease. *Ann. Neurol.* 46(6), 860–866 (1999).
12. Rowe CC, Ng S, Ackermann U *et al.* Imaging β-amyloid burden in aging and dementia. *Neurology* 68(20), 1718–1725 (2007).
13. Villemagne VL, Pike KE, Chetelat G *et al.* Longitudinal assessment of Aβ and cognition in aging and Alzheimer disease. *Ann. Neurol.* 69(1), 181–192 (2011).
14. Delaere P, Duyckaerts C, Masters C, Beyreuther K, Pierre F, Hauw JJ. Large amounts of neocortical β A4 deposits without neuritic plaques nor tangles in a psychometrically assessed, non-demented person. *Neurosci. Lett.* 116(1–2), 87–93 (1990).
15. Katzman R, Terry R, Deteresa R *et al.* Clinical, pathological, and neurochemical changes in dementia: a subgroup with preserved mental status and numerous neocortical plaques. *Ann. Neurol.* 23(2), 138–144 (1988).
16. Rowe CC, Ackerman U, Browne W *et al.* Imaging of amyloid β in Alzheimer's disease with ^{18}F-BAY94–9172, a novel PET tracer: proof of mechanism. *Lancet Neurol.* 7(2), 129–135 (2008).
17. Villemagne VL, Pike KE, Darby D *et al.* Aβ deposits in older non-demented individuals with cognitive decline are indicative of preclinical Alzheimer's disease. *Neuropsychologia* 46(6), 1688–1697 (2008).
18. Buee L, Bussiere T, Buee-Scherrer V, Delacourte A, Hof PR. Tau protein isoforms, phosphorylation and role in neurodegenerative disorders. *Brain Res. Brain Res. Rev.* 33(1), 95–130 (2000).
- ▪▪ **In-depth review of the characteristics of tau deposition.**
19. Braak E, Braak H, Mandelkow EM. A sequence of cytoskeleton changes related to the formation of neurofibrillary tangles and

neuropil threads. *Acta Neuropathol. (Berl.).* 87(6), 554–567 (1994).

20. Braak H, Braak E. Evolution of neuronal changes in the course of Alzheimer's disease. *J. Neural. Transm. Suppl.* 53, 127–140 (1998).
21. Braak H, Braak E. Staging of Alzheimer's disease-related neurofibrillary changes. *Neurobiol. Aging* 16(3), 271–278; discussion 278–284 (1995).
22. Delacourte A, David JP, Sergeant N *et al.* The biochemical pathway of neurofibrillary degeneration in aging and Alzheimer's disease. *Neurology* 52(6), 1158–1165 (1999).
23. Hanihara T, Amano N, Takahashi T, Nagatomo H, Yagashita S. Distribution of tangles and threads in the cerebral cortex in progressive supranuclear palsy. *Neuropathol. Appl. Neurobiol.* 21(4), 319–326 (1995).
24. Komori T. Tau-positive glial inclusions in progressive supranuclear palsy, corticobasal degeneration and Pick's disease. *Brain Pathol.* 9(4), 663–679 (1999).
25. Serrano-Pozo A, Mielke ML, Gomez-Isla T *et al.* Reactive glia not only associates with plaques but also parallels tangles in Alzheimer's disease. *Am. J. Pathol.* 179(3), 1373–1384 (2011).
26. Goedert M, Jakes R. Mutations causing neurodegenerative tau opathies. *Biochim. Biophys. Acta* 1739(2–3), 240–250 (2005).
27. Bugiani O. The many ways to frontotemporal degeneration and beyond. *Neurol. Sci.* 28(5), 241–244 (2007).
28. Mohorko N, Bresjanac M. Tau protein and human tauopathies: an overview. *Zdrav. Vestn.* 77(Suppl. 2). S35–S41 (2008).
29. Lee VM, Goedert M, Trojanowski JQ. Neurodegenerative tauopathies. *Annu. Rev. Neurosci.* 24, 1121–1159 (2001).
30. Mckee AC, Cantu RC, Nowinski CJ *et al.* Chronic traumatic encephalopathy in athletes: progressive tauopathy after repetitive head injury. *J. Neuropathol. Exp. Neurol.* 68(7), 709–735 (2009).
31. Delacourte A. Tauopathies: recent insights into old diseases. *Folia Neuropathol.* 43(4), 244–257 (2005).
32. Von Bergen M, Barghorn S, Li L *et al.* Mutations of tau protein in frontotemporal dementia promote aggregation of paired helical filaments by enhancing local β-structure. *J. Biol. Chem.* 276(51), 48165–48174 (2001).
33. Gotz J, Gladbach A, Pennanen L *et al.* Animal models reveal role for tau phosphorylation in human disease. *Biochim. Biophys. Acta* 1802(10), 860–871 (2010).
34. Roberson ED, Scearce-Levie K, Palop JJ *et al.* Reducing endogenous tau ameliorates amyloid β-induced deficits in an Alzheimer's disease mouse model. *Science* 316(5825), 750–754 (2007).
35. Chen F, David D, Ferrari A, Gotz J. Posttranslational modifications of tau – role in human tauopathies and modeling in transgenic animals. *Curr. Drug Targets* 5(6), 503–515 (2004).
36. Selenica ML, Jensen HS, Larsen AK *et al.* Efficacy of small-molecule glycogen synthase kinase-3 inhibitors in the postnatal rat model of tau hyperphosphorylation. *Br. J. Pharmacol.* 152(6), 959–979 (2007).
37. Giacobini E, Becker RE. One hundred years after the discovery of Alzheimer's disease. A turning point for therapy? *J. Alzheimers Dis.* 12(1), 37–52 (2007).
38. Tanaka T, Zhong J, Iqbal K, Trenkner E, Grundke-Iqbal I. The regulation of phosphorylation of tau in SY5Y neuroblastoma cells: the role of protein phosphatases. *FEBS Lett.* 426(2), 248–254 (1998).
39. Zhang B, Maiti A, Shively S *et al.* Microtubule-binding drugs offset tau sequestration by stabilizing microtubules and reversing fast axonal transport deficits in a tauopathy model. *Proc. Natl Acad. Sci. USA* 102(1), 227–231 (2005).
40. Matsuoka Y, Jouroukhin Y, Gray AJ *et al.* A neuronal microtubule interacting agent, NAP, reduces tau pathology and enhances cognitive function in a mouse model of Alzheimer's disease. *J. Pharmacol. Exp. Ther.* 325(1), 146–153 (2008).
41. Asuni AA, Boutajangout A, Quartermain D, Sigurdsson EM. Immunotherapy targeting pathological tau conformers in a tangle mouse model reduces brain pathology with associated functional improvements. *J. Neurosci.* 27(34), 9115–9129 (2007).
42. Wischik CM, Edwards PC, Lai RY, Roth M, Harrington CR. Selective inhibition of Alzheimer disease-like tau aggregation by phenothiazines. *Proc. Natl Acad. Sci. USA* 93(20), 11213–11218 (1996).
43. Brunden KR, Zhang B, Carroll J *et al.* Epothilone D improves microtubule density, axonal integrity, and cognition in a transgenic mouse model of tauopathy. *J. Neurosci.* 30(41), 13861–13866 (2010).
44. Klunk WE, Lopresti BJ, Ikonomovic MD *et al.* Binding of the positron emission tomography tracer Pittsburgh compound-B reflects the amount of amyloid-β in Alzheimer's disease brain but not in transgenic mouse brain. *J. Neurosci.* 25(46), 10598–10606 (2005).
45. Agdeppa ED, Kepe V, Liu J *et al.* Binding characteristics of radiofluorinated 6-dialkylamino-2-naphthylethylidene derivatives as positron emission tomography imaging probes for β-amyloid plaques in Alzheimer's disease. *J. Neurosci.* 21(24), RC189 (2001).
46. Thompson PW, Ye L, Morgenstern JL *et al.* Interaction of the amyloid imaging tracer FDDNP with hallmark Alzheimer's disease pathologies. *J. Neurochem.* 109(2), 623–630 (2009).
47. Maas T, Eidenmuller J, Brandt R. Interaction of tau with the neural membrane cortex is regulated by phosphorylation at sites that are modified in paired helical filaments. *J. Biol. Chem.* 275(21), 15733–15740 (2000).
48. Hernandez F, Avila J. Tauopathies. *Cell Mol. Life Sci.* 64(17), 2219–2233 (2007).
49. Arima K. Ultrastructural characteristics of tau filaments in tau opathies: immuno-electron microscopic demonstration of tau filaments in tauopathies. *Neuropathology* 26(5), 475–483 (2006).
50. Mulholland GK, Wieland DM, Kilbourn MR *et al.* [^{18}F]fluoroethoxy-benzovesamicol, a PET radiotracer for the vesicular acetylcholine transporter and cholinergic synapses. *Synapse* 30(3), 263–274 (1998).
51. Vander Borght TM, Kilbourn MR, Koeppe RA *et al. In vivo* imaging of the brain vesicular monoamine transporter. *J. Nucl. Med.* 36(12), 2252–2260 (1995).
52. Villemagne VL, Okamura N, Pejoska S *et al. In vivo* assessment of vesicular monoamine transporter type 2 in dementia with Lewy bodies and Alzheimer disease. *Arch. Neurol.* 68(7), 905–912 (2011).
53. Takahashi K, Bergstrom M, Frandberg P, Vesstrom EL, Watanabe Y, Langstrom B. Imaging of aromatase distribution in rat and rhesus monkey brains with [^{11}C]vorozole. *Nucl. Med. Biol.* 33(5), 599–605 (2006).
54. Biegon A, Kim SW, Alexoff DL *et al.* Unique distribution of aromatase in the human brain: *in vivo* studies with PET and [*N*-methyl-^{11}C] vorozole. *Synapse* 64(11), 801–807 (2010).
55. Sergeant N, Bretteville A, Hamdane M *et al.* Biochemistry of tau in Alzheimer's disease and related neurological disorders. *Expert Rev. Proteomics* 5(2), 207–224 (2008).

▪▪ **In-depth review of tauopathies.**

56. Goedert M, Spillantini MG, Potier MC, Ulrich J, Crowther RA. Cloning and sequencing of the cDNA encoding an isoform of microtubule-associated protein tau containing four tandem repeats: differential expression of tau protein mRNAs in human brain. *EMBO J.* 8(2), 393–399 (1989).
57. Andreadis A, Broderick JA, Kosik KS. Relative exon affinities and suboptimal splice site signals lead to non-equivalence of two

cassette exons. *Nucleic Acids Res.* 23(17), 3585–3593 (1995).

58. Bunker JM, Wilson L, Jordan MA, Feinstein SC. Modulation of microtubule dynamics by tau in living cells: implications for development and neurodegeneration. *Mol. Biol. Cell* 15(6), 2720–2728 (2004).

60. Levy SF, Leboeuf AC, Massie MR, Jordan MA, Wilson L, Feinstein SC. Three- and four-repeat tau regulate the dynamic instability of two distinct microtubule subpopulations in qualitatively different manners. Implications for neurodegeneration. *J. Biol. Chem.* 280(14), 13520–13528 (2005).

61. Sergeant N, Delacourte A, Buee L. Tau protein as a differential biomarker of tauopathies. *Biochim. Biophys. Acta* 1739(2–3), 179–197 (2005).

62. King ME, Ghoshal N, Wall JS, Binder LI, Ksiezak-Reding H. Structural analysis of Pick's disease-derived and *in vitro*-assembled tau filaments. *Am. J. Pathol.* 158(4), 1481–1490 (2001).

63. Scaravilli T, Tolosa E, Ferrer I. Progressive supranuclear palsy and corticobasal degeneration: lumping versus splitting. *Mov. Disord.* 20(Suppl. 12), S21–S28 (2005).

64. Uchihara T, Tsuchiya K. Neuropathology of pick body disease. In: *Handbook of Clinical Neurology (3rd Series) Dementias*. Duyckaerts C, Litvan I (Eds). Elsevier, Amsterdam, The Netherlands, 415–430 (2008).

65. Delacourte A, Buee L. Tau pathology: a marker of neurodegenerative disorders. *Curr. Opin. Neurol.* 13(4), 371–376 (2000).

66. Wegmann S, Jung YJ, Chinnathambi S, Mandelkow EM, Mandelkow E, Muller DJ. Human tau isoforms assemble into ribbon-like fibrils that display polymorphic structure and stability. *J. Biol. Chem.* 285(35), 27302–27313 (2010).

67. Von Bergen M, Barghorn S, Biernat J, Mandelkow EM, Mandelkow E. Tau aggregation is driven by a transition from random coil to β sheet structure. *Biochim. Biophys. Acta* 1739(2–3), 158–166 (2005).

68. Chirita CN, Congdon EE, Yin H, Kuret J. Triggers of full-length tau aggregation: a role for partially folded intermediates. *Biochemistry* 44(15), 5862–5872 (2005).

▪▪ **In-depth review of the multiple post-translational modifications of tau protein.**

68. Martin L, Latypova X, Terro F. Post-translational modifications of tau protein: implications for Alzheimer's disease. *Neurochem. Int.* 58(4), 458–471 (2011).

70. Levine H 3rd, Walker LC. Molecular polymorphism of Aβ in Alzheimer's disease. *Neurobiol. Aging* 31(4), 542–548 (2010).

71. Rosen RF, Walker LC, Levine H 3rd. PIB binding in aged primate brain: enrichment of high-affinity sites in humans with Alzheimer's disease. *Neurobiol. Aging* 32(2), 223–234 (2011).

72. Forman MS, Zhukareva V, Bergeron C *et al.* Signature tau neuropathology in gray and white matter of corticobasal degeneration. *Am. J. Pathol.* 160(6), 2045–2053 (2002).

73. Khatoon S, Grundke-Iqbal I, Iqbal K. Levels of normal and abnormally phosphorylated tau in different cellular and regional compartments of Alzheimer disease and control brains. *FEBS Lett.* 351(1), 80–84 (1994).

74. Mukaetova-Ladinska EB, Harrington CR, Roth M, Wischik CM. Biochemical and anatomical redistribution of tau protein in Alzheimer's disease. *Am. J. Pathol.* 143(2), 565–578 (1993).

▪ **Thorough assessment of the regional PHF-tau concentration in the brain.**

75. Wischik C, Harrington C, Mukaetova-Ladinska EB. Molecular characterization of the neurodegenerative changes which distinguishes normal ageing from Alzheimer's disease. In: *Dementia and Normal Ageing*. Huppert FA, Brayne C, O'connor DW (Eds). Cambridge University Press, New York, USA 470–491 (1994).

76. Zhukareva V, Mann D, Pickering-Brown S *et al.* Sporadic Pick's disease: a tauopathy characterized by a spectrum of pathological tau isoforms in gray and white matter. *Ann. Neurol.* 51(6), 730–739 (2002).

77. Kovacs GG, Majtenyi K, Spina S *et al.* White matter tauopathy with globular glial inclusions: a distinct sporadic frontotemporal lobar degeneration. *J. Neuropathol. Exp. Neurol.* 67(10), 963–975 (2008).

78. Fodero-Tavoletti MT, Rowe CC, Mclean CA *et al.* Characterization of PiB binding to white matter in Alzheimer disease and other dementias. *J. Nucl. Med.* 50(2), 198–204 (2009).

79. Chou YC, Teng MM, Guo WY, Hsieh JC, Wu YT. Classification of hemodynamics from dynamic-susceptibility-contrast magnetic resonance (DSC-MR) brain images using noiseless independent factor analysis. *Med. Image Anal.* 11(3), 242–253 (2007).

80. Liu P, Uh J, Devous MD, Adinoff B, Lu H. Comparison of relative cerebral blood flow maps using pseudo-continuous arterial spin labeling and single photon emission computed tomography. *NMR Biomed.* 25(5), 779–786 (2011)

81. Klunk WE, Wang Y, Huang GF *et al.* The binding of 2-(4'-methylaminophenyl) benzothiazole to postmortem brain homogenates is dominated by the amyloid component. *J. Neurosci.* 23(6), 2086–2092 (2003).

82. Lockhart A, Lamb JR, Osredkar T *et al.* PIB is a non-specific imaging marker of amyloid-β (Aβ) peptide-related cerebral amyloidosis. *Brain* 130(Pt 10), 2607–2615 (2007).

83. Ikonomovic MD, Klunk WE, Abrahamson EE *et al.* Post-mortem correlates of *in vivo* PiB-PET amyloid imaging in a typical case of Alzheimer's disease. *Brain* 131(Pt 6), 1630–1645 (2008).

84. Fodero-Tavoletti MT, Smith DP, Mclean CA *et al.* *In vitro* characterization of Pittsburgh compound-B binding to Lewy bodies. *J. Neurosci.* 27(39), 10365–10371 (2007).

85. Ye L, Velasco A, Fraser G *et al.* *In vitro* high affinity α-synuclein binding sites for the amyloid imaging agent PIB are not matched by binding to Lewy bodies in postmortem human brain. *J. Neurochem.* 105(4), 1428–1437 (2008).

86. Naslund J, Haroutunian V, Mohs R *et al.* Correlation between elevated levels of amyloid β-peptide in the brain and cognitive decline. *JAMA* 283(12), 1571–1577 (2000).

▪ **Thorough assessment of the regional Aβ concentration in the brain.**

87. Lyon RA, Titeler M, Frost JJ *et al.* ^{3}H-3-*N*-methylspiperone labels D2 dopamine receptors in basal ganglia and S2 serotonin receptors in cerebral cortex. *J. Neurosci.* 6(10), 2941–2949 (1986).

88. Heiss WD, Herholz K. Brain receptor imaging. *J. Nucl. Med.* 47(2), 302–312 (2006).

89. Villemagne VL, Fodero-Tavoletti MT, Pike KE, Cappai R, Masters CL, Rowe CC. The ART of loss: Aβ imaging in the evaluation of Alzheimer's disease and other dementias. *Mol. Neurobiol.* 38(1), 1–15 (2008).

▪ **Review on Aβ imaging in Alzheimer's disease.**

90. Laruelle M, Slifstein M, Huang Y. Relationships between radiotracer properties and image quality in molecular imaging of the brain with positron emission tomography. *Mol. Imaging Biol.* 5(6), 363–375 (2003).

▪ **Review on the general requirements for neuroimaging radiotracers.**

91. Pike VW. PET radiotracers: crossing the blood–brain barrier and surviving metabolism. *Trends Pharmacol. Sci.* 30(8), 431–440 (2009).

▪ **Review of some aspects to be considered in radiotracer design.**

92. Pardridge WM. Drug and gene delivery to the brain: the vascular route. *Neuron* 36(4),

555–558 (2002).

93. Villemagne VL, Rowe CC. Amyloid ligands for dementia. *PET Clin.* 5, 33–53 (2010).
94. Keng PY, Esterby M, Van Dam RM. Emerging technologies for decentralized production of PET tracers. In: *Positron Emission Tomography – Current Clinical and Research Aspects*. Hsieh CH (Ed.). InTech, Rijeka, Croatia 153–182 (2012).
95. Ruth T. Accelerating production of medical isotopes. *Nature* 457(7229), 536–537 (2009).
96. Ponto JA, Hung JC. Nuclear pharmacy, Part II: nuclear pharmacy practice today. *J. Nucl. Med. Technol.* 28(2), 76–81, Quiz 83 (2000).
97. Mintun MA, Raichle ME, Kilbourn MR, Wooten GF, Welch MJ. A quantitative model for the *in vivo* assessment of drug binding sites with positron emission tomography. *Ann. Neurol.* 15(3), 217–227 (1984).
98. Fodero-Tavoletti MT, Okamura N, Furumoto S *et al.* ^{18}F-THK523: a novel *in vivo* tau imaging ligand for Alzheimer's disease. *Brain* 134(Pt 4), 1089–1100 (2011).
99. Rojo LE, Alzate-Morales J, Saavedra IN, Davies P, Maccioni RB. Selective interaction of lansoprazole and astemizole with tau polymers: potential new clinical use in diagnosis of Alzheimer's disease. *J. Alzheimers Dis.* 19(2), 573–589 (2010).
100. Prabhakaran J, Majo VJ, Milak MS *et al.* Synthesis, *in vitro* and *in vivo* evaluation of [^{11}C]MMTP: a potential PET ligand for mGluR1 receptors. *Bioorg. Med. Chem. Lett.* 20(12), 3499–3501 (2010).
101. Choi SR, Golding G, Zhuang Z *et al.* Preclinical properties of ^{18}F-AV-45: a PET agent for Aβ plaques in the brain. *J. Nucl. Med.* 50(11), 1887–1894 (2009).
102. Honson NS, Johnson RL, Huang W, Inglese J, Austin CP, Kuret J. Differentiating Alzheimer disease-associated aggregates with small molecules. *Neurobiol. Dis.* 28(3), 251–260 (2007).
103. Okamura N, Suemoto T, Furumoto S *et al.* Quinoline and benzimidazole derivatives: candidate probes for *in vivo* imaging of tau pathology in Alzheimer's disease. *J. Neurosci.* 25(47), 10857–10862 (2005).
104. Schafer KN, Kim S, Matzavinos A, Kuret J. Selectivity requirements for diagnostic imaging of neurofibrillary lesions in Alzheimer's disease: a simulation study. *Neuroimage* 60(3), 1724–1733 (2012).
105. Smith DA, Jones BC, Walker DK. Design of drugs involving the concepts and theories of drug metabolism and pharmacokinetics. *Med. Res. Rev.* 16(3), 243–266 (1996).
106. Dishino DD, Welch MJ, Kilbourn MR, Raichle ME. Relationship between lipophilicity and brain extraction of C-11-labeled radiopharmaceuticals. *J. Nucl. Med.* 24(11), 1030–1038 (1983).
107. Zhang Y, Pavlova OA, Chefer SI *et al.* 5-substituted derivatives of 6-halogeno-3-((2-(S)-azetidinyl)methoxy)pyridine and 6-halogeno-3-((2-(S)-pyrrolidinyl)methoxy) pyridine with low picomolar affinity for α4β2 nicotinic acetylcholine receptor and wide range of lipophilicity: potential probes for imaging with positron emission tomography. *J. Med. Chem.* 47(10), 2453–2465 (2004).
108. Sihver W, Langstrom B, Nordberg A. Ligands for *in vivo* imaging of nicotinic receptor subtypes in Alzheimer brain. *Acta Neurol. Scand. Suppl.* 176, 27–33 (2000).
109. Klunk WE, Price JC, Mathis CA *et al.* Amyloid deposition begins in the striatum of presenilin-1 mutation carriers from two unrelated pedigrees. *J. Neurosci.* 27(23), 6174–6184 (2007).
110. Tomiyama T, Nagata T, Shimada H *et al.* A new amyloid β variant favoring oligomerization in Alzheimer's-type dementia. *Ann. Neurol.* 63(3), 377–387 (2008).
111. Cairns NJ, Ikonomovic MD, Benzinger T *et al.* Absence of Pittsburgh compound B detection of cerebral amyloid β in a patient with clinical, cognitive, and cerebrospinal fluid markers of Alzheimer disease. *Arch. Neurol.* 66(12), 1557–1562 (2009).
112. Klunk WE, Engler H, Nordberg A *et al.* Imaging brain amyloid in Alzheimer's disease with Pittsburgh compound-B. *Ann. Neurol.* 55(3), 306–319 (2004).
113. Taghavi A, Nasir S, Pickhardt M *et al.* N'-benzylidene-benzohydrazides as novel and selective tau -PHF ligands. *J. Alzheimers Dis.* 27(4), 835–843 (2011).
114. Honson NS, Jensen JR, Darby MV, Kuret J. Potent inhibition of tau fibrillization with a multivalent ligand. *Biochem. Biophys. Res. Commun.* 363(1), 229–234 (2007).
115. Wischik C, Staff R. Challenges in the conduct of disease-modifying trials in AD: practical experience from a Phase 2 trial of tau-aggregation inhibitor therapy. *J. Nutr. Health Aging* 13(4), 367–369 (2009).
116. Jensen JR, Cisek K, Funk KE, Naphade S, Schafer KN, Kuret J. Research towards tau imaging. *J. Alzheimers Dis.* 26(Suppl. 3), 147–157 (2011).
117. Kudo Y. Development of amyloid imaging PET probes for an early diagnosis of Alzheimer's disease. *Minim. Invasive Ther. Allied Technol.* 15(4), 209–213 (2006).
118. Jack CR Jr, Knopman DS, Jagust WJ *et al.* Hypothetical model of dynamic biomarkers of the Alzheimer's pathological cascade. *Lancet Neurol.* 9(1), 119–128 (2010).
119. Jack CR Jr, Lowe VJ, Senjem ML *et al.* ^{11}C PiB and structural MRI provide complementary information in imaging of Alzheimer's disease and amnestic mild cognitive impairment. *Brain* 131(Pt 3), 665–680 (2008).
120. Hampel H, Ewers M, Burger K *et al.* Lithium trial in Alzheimer's disease: a randomized, single-blind, placebo-controlled, multicenter 10-week study. *J. Clin. Psychiatry* 70(6), 922–931 (2009).
121. Gozes I, Stewart A, Morimoto B, Fox A, Sutherland K, Schmeche D. Addressing Alzheimer's disease tangles: from NAP to AL-108. *Curr. Alzheimer Res.* 6(5), 455–460 (2009).

Patents

201. Kemp S, Storey L, Storey J, Rickard J, Harrington C, Wischik C. Ligands for aggregated tau molecules: 2010/034982 (2010).
202. Kudo Y, Furumoto S, Okamura N. Benzoxazole derivatives: 2010/0021385 (2010).
203. Szardenings AK, Zhang W, Kolb HC *et al.* Siemens Medical Solutions USA, Inc. Imaging agents for detecting neurological disorders: 2011/0182812 A1(2011).
204. Kudo Y, Susuki M, Suemoto T *et al.* Quinoline derivative as diagnostic probe for disease with tau protein accumulation: 7,118,730 (2006).

Circulation
JOURNAL OF THE AMERICAN HEART ASSOCIATION

American Heart Association®

Cardiac Positron-Emission Tomography Images With an Amyloid-Specific Tracer in Familial Transthyretin-Related Systemic Amyloidosis

Katsutoshi Furukawa, Shu-ichi Ikeda, Nobuyuki Okamura, Manabu Tashiro, Naoki Tomita, Shozo Furumoto, Ren Iwata, Kazuhiko Yanai, Yukitsuka Kudo and Hiroyuki Arai

Circulation. 2012;125:556-557
doi: 10.1161/CIRCULATIONAHA.111.045237
Circulation is published by the American Heart Association, 7272 Greenville Avenue, Dallas, TX 75231

Print ISSN: 0009-7322. Online ISSN: 1524-4539

Cardiac Positron-Emission Tomography Images With an Amyloid-Specific Tracer in Familial Transthyretin-Related Systemic Amyloidosis

Katsutoshi Furukawa, MD, PhD; Shu-ichi Ikeda, MD, PhD; Nobuyuki Okamura, MD, PhD; Manabu Tashiro, MD, PhD; Naoki Tomita, MD, PhD; Shozo Furumoto, PhD; Ren Iwata, PhD; Kazuhiko Yanai, MD, PhD; Yukitsuka Kudo, PhD; Hiroyuki Arai, MD, PhD

We report the case of a 32-year-old man who had suffered from orthostatic syncope and body weight loss since he was 27 years old. As years passed by, he also showed muscle weakness and abnormal sensations in both legs, hyporeflexia in 4 limbs, and autonomic failure (impotence, urinary and fecal incontinence, and edema in lower limbs) suggesting the presence of peripheral somatic and autonomic polyneuropathy. His mother, mother's father, and mother's paternal aunt also had similar symptoms. Both the sensory nerve action potential and the sensory nerve conduction velocity of his right sural nerve were low (1.26 μV and 47.2 m/s, respectively), and the motor nerve conduction velocity of his right tibial nerve was 41.1 m/s (normal >45 m/s). A DNA test on the man disclosed a missense mutation in the transthyretin gene (Ser50Arg), which is relatively rare in familial transthyretin-related systemic amyloidosis.[1,2] Transthyretin-immunoreactive amyloid deposition was demonstrated in the biopsied gastroduodenal mucosa (Figure 1). Echocardiography showed a markedly thickened ventricular wall (thickness of interventricular septum 22.3 mm [normal <12 mm]) with normal wall motion (fractional shortening 37.6% [normal 28–42%]), indicating that he also had cardiac

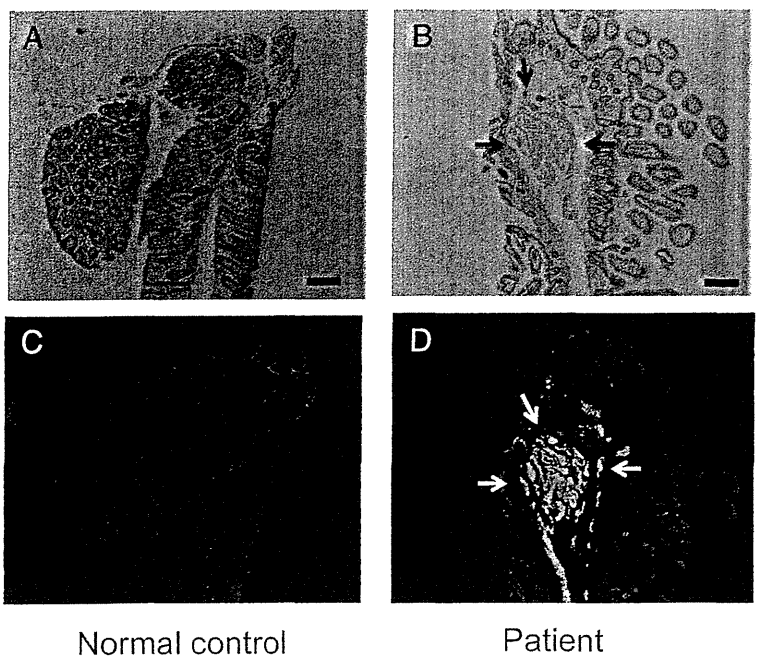

Figure 1. Detection of amyloid deposition in the intestines. Congo red (**A** and **B**) and BF-227 (**C** and **D**) clearly detect transthyretin in the submucosal space of the small intestine of the patient. Scale bars, 100 μm.

From the Department of Geriatrics and Gerontology, Division of Brain Sciences, Institute of Development, Aging and Cancer, Tohoku University (K.F., N.T., H.A.); Department of Medicine (Neurology & Rheumatology), Shinshu University School of Medicine (S.I.); Department of Pharmacology, Tohoku University Graduate School of Medicine (N.O., S.F., K.Y.); Division of Cyclotron Nuclear Medicine, Cyclotron and Radioisotope Center, Tohoku University (M.T.); Division of Radiopharmaceutical Chemistry, Cyclotron and Radioisotope Center, Tohoku University (R.I.); Department of NeuroImaging Research, Innovation New Biomedical Engineering Center, Tohoku University (Y.K.), Sendai, Japan.

Correspondence to Katsutoshi Furukawa, MD, PhD, Department of Geriatrics and Gerontology, Institute of Development, Aging and Cancer, Tohoku University, 4-1 Seiryo-machi Aobaku, Sendai 980-8575 Japan. E-mail kfurukawa-ns@umin.ac.jp

(*Circulation*. 2012;125:556-557.)

Circulation is available at http://circ.ahajournals.org

DOI: 10.1161/CIRCULATIONAHA.111.045237

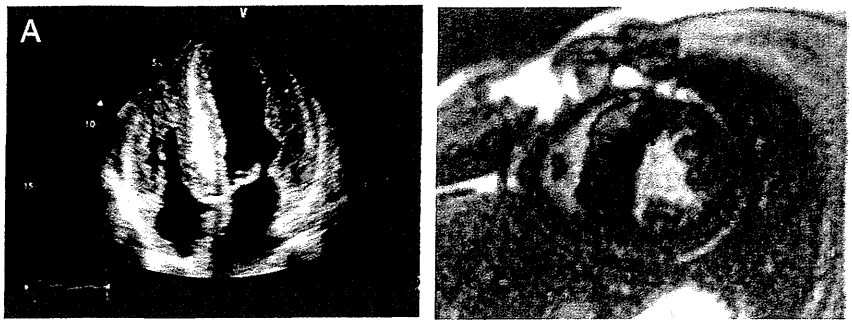

Figure 2. A, Echocardiographic finding. Four chamber views show symmetrical thickening of ventricular walls and septum with hyperrefractile myocardial echo (the so-called granular sparkling appearance). **B**, Contrast magnetic resonance imaging with gadolinium. Focal late gadolinium enhancement is visible (arrows).

amyloidosis (Figure 2A). Contrast magnetic resonance imaging[3] revealed focal late gadolinium enhancement in the thickened ventricular wall (Figure 2B). The patient had been treated with orthotopic live-donor liver transplantation when he was 31 years old to alleviate and prevent exacerbation of his neuronal and cardiac symptoms. His condition, including the neurological disability, gradually improved, and he started to work again 10 months after liver transplantation.

In order to visualize amyloid deposition in the myocardium, the patient underwent a cardiac positron-emission tomography study with [^{11}C]-BF-227 that sensitively and specifically binds to aggregated amyloid fibrils.[4] The positron-emission tomography images revealed significantly robust retention of [^{11}C]-BF-227 in the patient's heart compared with that of the normal control (Figure 3). Biopsy specimens from the patient's duodenum also showed higher signals of BF-227 compared with that of the normal control (Figure 1, C and D). The present result provides evidence that our amyloid-specific positron-emission tomography tracer, [^{11}C]-BF-227, can successfully detect amyloid deposition in the heart. Several molecules, such as ^{99m}Tc-aprotinin and ^{99m}Tc-labeled phosphate derivatives, have been investigated to visualize cardiac amyloidosis.[2] None of the previous tracers, however, could specifically bind to aggregated amyloid, which forms a β-pleated sheet structure. In any of the amyloidgenic disorders, such as transthyretin-related systemic amyloidosis and Alzheimer's disease, it is surmised that the monomer of the amyloid protein itself is not very toxic, whereas misfolded oligomers could cause damage to human organs.[1-4] It is therefore truly important to detect the accumulation of real amyloid fibrils for the early and accurate diagnosis of amyloidosis. To our knowledge, this is the first report showing the usefulness of a β-pleated sheet structure-specific positron-emission tomography in investing visceral organ amyloidosis.

Sources of Funding

This study was supported by the Program for the Promotion of Fundamental Studies in Health Science by the National Institute of Biomedical Innovation; the Special Coordination Funds for Promoting Science and Technology; the Industrial Technology Research Grant Program from the New Energy and Industrial Technology Development Organization of Japan; Health and Labor Sciences Research Grants for Translational Research from the Ministry of Health; and the Ministry of Education, Culture, Sports and Technology of Japan.

Acknowledgments

We appreciate technical assistance of Shoichi Watanuki, Yoichi Ishikawa, Motohisa Kato, and Emiko Fukuda.

Disclosures

None.

References

1. Ikeda S, Nakazato M, Ando Y, Sobue G. Familial transthyretin-type amyloid polyneuropathy in Japan: Clinical and genetic heterogeneity. *Neurology*. 2002;58:1001–1007.
2. Rapezzi C, Quarta CC, Riva L, Longhi S, Gallelli I, Lorenzini M, Ciliberti P, Biagini E, Salvi F, Branzi A. Transthyretin-related amyloidoses and the heart: a clinical overview. *Nat Rev Cardiol*. 2010;7:398–408.
3. Vogelsberg H, Mahrholdt H, Deluigi CC, Yilmaz A, Kispert Eva M, Greulich S, Klingel K, Kandolf R, Sechtem U. Cardiovascular magnetic resonance in clinically suspected cardiac amyloidosis. *J Am Coll Cardiol*. 2008;s51:1022–1030.
4. Furukawa K, Okamura N, Tashiro M, Waragai M, Furumoto S, Iwata R, Yanai K, Kudo Y, Arai H. Amyloid PET in mild cognitive impairment and Alzheimer's disease with BF-227: Comparison to FDG-PET. *J Neurol*. 2010;257:721–727.

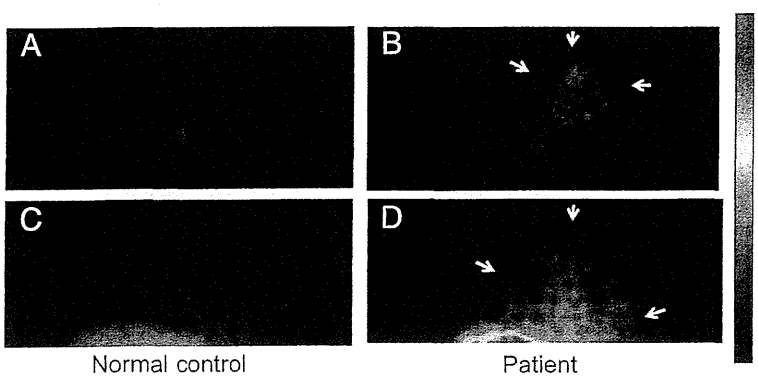

Figure 3. [^{11}C]-BF-227 positron emission tomgraphy succeeds in visualization of amyloid deposition in the heart. Axial and coronal images are **A** and **B** and **C** and **D**, respectively. Arrows indicate high signals of [^{11}C]-BF-227 in the heart of the patient (**B** and **D**).

別冊日本臨牀　新領域別症候群シリーズ　No.23　(2013年5月20日発行) 別刷

血液症候群(第2版)

—その他の血液疾患を含めて—

III

X　血漿タンパクの異常

アミロイドーシス

局所性アミロイドーシス

脳アミロイドーシス

工藤幸司
荒井啓行

X 血漿タンパクの異常

アミロイドーシス
局所性アミロイドーシス

脳アミロイドーシス

Cerebral amyloidosis

工藤幸司[1]
荒井啓行[2]

Key words：脳アミロイドーシス，アルツハイマー病，preclinical AD

はじめに

脳アミロイドーシス(cerebral amyloidosis)とは脳へのアミロイド沈着が認められる疾患であり，沈着するアミロイドにより疾患特性が存在する．例えばアミロイドβタンパク(Aβ)は，アルツハイマー病(Alzheimer's disease: AD)および脳アミロイドアンギオパチー(cerebral amyloid angiopathy: CAA)において，また異常型プリオンタンパクはプリオン病(prion disease)においてそれぞれ観察される．

本稿では，主としてADにつき述べてみたい．

1. アルツハイマー病(AD)

ADにおける近年の話題で最も我々を驚かせたのは2010年7月ハワイで開催された国際アルツハイマー病学会(International Conference on Alzheimer's Disease 2010: ICAD2010)において，アメリカの2つの機関，すなわちNational Institute on Aging(NIA)とAlzheimer's Association(AA)から提案された新しいAD診断基準であったことに，異を唱えるAD研究者は少ないであろう．両機関はADをpreclinical AD，MCI due to ADおよびAD dementiaの3つの時期に分け，それぞれに新しい診断基準を提案した(提案の最終バージョンは2011年に公表)[1-4]．それらの提案の中で我々が驚かされたその本体は，臨床症状が認められなくてもAD特有の病理像を検出できたらpreclinical AD[4]として病気に組み入れるという新しい概念を提示されたことであった(ただし，この概念はあくまでもresearch criteriaとのこと)．学会でこれを最初に聞いたときは，'あっ，またアメリカに負けた！日本の社会ではこのような概念は提案できないだろうし，受け入れられないだろうなあ．これで彼らはまたまた日本の前を走り続けるのだろうなあ'が感想であった．

2011年に公表されたpreclinical ADに関する文献[4]の内容を紹介すると，**図1**は主としてpreclinical ADにおけるバイオマーカーとそれらのスタート時点およびその後の経過を示しているが，ADのバイオマーカーとして最も初期(stage 1)に検出できるそれはAβである．具体的なバイオマーカーとしては，アミロイドイメージング用陽電子断層撮影装置(positron emission tomography: PET)プローブとPETによって判明する主として患者脳灰白質におけるAβ蓄積量の増加，および脳脊髄液中のAβ1-42の低下である．preclinical ADを更に詳しく定義しているのが**表1**(文献[4]には記載されていない．2010年秋頃NIAおよびAAのホームページからリンクできたが，現時点では不可能)である．これにはpreclinical ADのstage 1はasymptomatic cerebral amyloidosisと記載されており，更に同表から各stageにおけるバイオマーカーの詳細を追跡することができる．

両機関がこの提案，特にpreclinical ADという新しい概念を導入するに至った経緯について，

[1]Yukitsuka Kudo, [2]Hiroyuki Arai: [1]Clinical Research, Innovation and Education Center, Tohoku University Hospital 東北大学病院 臨床試験推進センター [2]Institute of Development, Aging and Cancer, Tohoku University 東北大学加齢医学研究所

0047-1852/13/¥60/頁/JCOPY

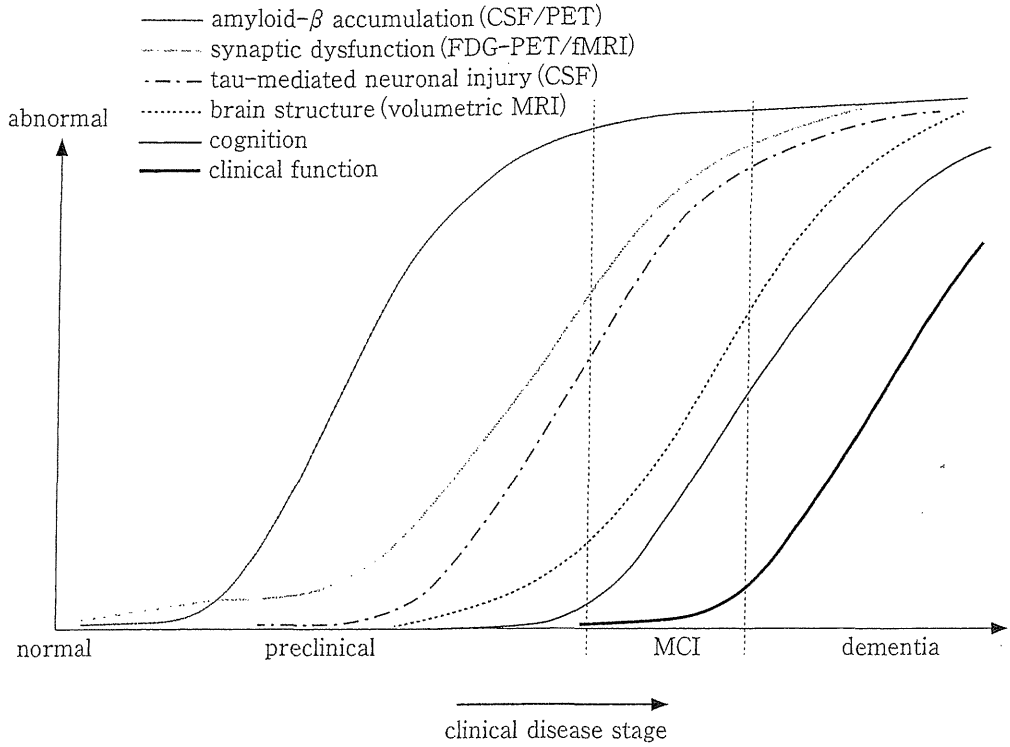

図1 アルツハイマー病，特に **preclinical AD** におけるバイオマーカーとそれらの発現時期(文献[4]より引用)

著者らは以下のように推察している．2008年6月以降，セクレターゼ阻害薬類，ワクチン，抗体をはじめとするいわゆる根本治療薬の治験成績が次々と公表された．多くの研究者，臨床家はこれらの介入によって少なくとも臨床症状の進行はストップする，と予測していたものと思われるが，それらの結果は我々の期待を大きく裏切るものであった．その中でも特に落胆させられたのはAβワクチンによって脳内Aβがクリアーされた患者においても，認知症の進行は食い止めることができなかったという2008年，Lancetの報告であった[5]．

これらの成績をどのように解釈するかであるが，まずこれらの薬物はADの治療薬とはなりえないとする立場をとるのが一般的と考えられる．一方，Aβの蓄積が始まる極めて早期にこれらの薬物を処方したならばADの一連の病理像の連鎖をスタート時点(=Aβ蓄積スタート時点)付近で断つことができ，その後のAD発症を抑制できる可能性があると推測することもできる．近年，この推測が正しいかもしれないことが示唆される報告も散見されている．すなわち，抗Aβ抗体bapineuzumab[6]やgantenerumab[7]により脳内Aβは減少することがアミロイドイメージング用PETプローブ[^{11}C]PiBを用いた試験によって確かめられており，また抗Aβ抗体solanezumabでは軽度のADにおいて認知機能低下の進行抑制(進行のストップではない)が認められたとのプレス発表がなされている[日本イーライリリー：https://www.lilly.co.jp/pressrelease/2012/news_2012_135.aspx].

2. Preclinical ADとアミロイドイメージング

臨床症状の全くみられないpreclinical ADを拾い上げるためには，現時点では**図1**および**表1**のstage 1に示されているように脳内Aβをを PETで画像化するか，または脳脊髄液中のAβ1-42の低下を指標にするかであるが，本稿では前者について概説したい．

脳内Aβ蓄積を画像化するためには，いわゆるアミロイドイメージング用PETプローブが

表1　National Institute on Aging(NIA)およびAlzheimer's Association(AA)提案によるpreclinical ADの診断基準

Operational Research Criteria for Defining Preclinical AD

1. biomarker evidence of amyloid-β accumulation(stage 1=asymptomatic cerebral amyloidosis)
   a. elevated tracer retention on PET amyloid imaging and/or low $A\beta_{42}$ on CSF assay
2. biomarker evidence of synaptic dysfunction and/or early neurodegeneration(stage 2=evidence of amyloid positivity+presence of one or more additional AD markers)
   a. elevated CSF tau or phospho-tau
   b. hypometabolism in an AD-like pattern(i.e. posterior cingulate, precuneus, and/or temporo-parietal cortices) on FDG-PET
   c. cortical thinning/grey matter loss in AD-like anatomic distribution(i.e. lateral and medial parietal, posterior cingulate and lateral temporal cortices) and/or hippocampal atrophy on volumetric MRI
3. evidence of subtle cognitive decline, but does not meet criteria for MCI or dementia (stage 3=amyloid positivity+markers of neurodegeneration+very early cognitive symptoms)
   a. demonstrated cognitive decline over time on standard cognitive tests, but not meeting criteria for MCI
   b. subtle impairment on challenging cognitive tests, particularly accounting for level of innate ability or cognitive reserve but not meeting criteria for MCI

必要であるが，これらの中で最も使用頻度の高いプローブはピッツバーグ大学Klunkら—General Electric社の[^{11}C]PiBである．アミロイドイメージングはAD診断の強力なツールとして認められつつあるが，一方では想定外のデータも得られた．それを[^{11}C]PiBを例に紹介すると，2008年7月シカゴでの国際アルツハイマー病学会に先駆けて開催されたADNI(Alzheimer's Disease Neuroimaging Initiative) meetingにおいて健常高齢者の53％が[^{11}C]PiB陽性者であったという驚くべき報告がなされた．AD発症率は65歳以上人口の4-6％と考えられているが，ADNIの報告はADおよびMCI患者を除いた高齢者の53％が[^{11}C]PiB陽性であったということである．また2009年11月，仙台での第28回日本認知症学会に引き続き開催された'World Wide ADNIの展望'においても，特にアメリカでの健常高齢者の約40％が[^{11}C]PiB陽性とのことであった．これら以外にも多くの報告で健常高齢者における無視できない[^{11}C]PiB陽性者が存在することが確かめられている．

なぜこのような問題点が浮き彫りにされるかについては，以下のように説明できると著者らは考えている．すなわち健常高齢者，MCIおよびAD患者のいずれにおいてもAβ蓄積にはかなりのばらつきが存在するために，言い換えると健常高齢者においてもMCIおよびAD患者を凌ぐ，またMCI患者においてもAD患者を凌ぐAβ蓄積を示す個体が無視できない割合で存在するために多くの偽陽性者がみられ，プローブの集積と認知症尺度との間に相関がみられないのであろう．

ここまで書いてきたら次の予想がつくのかもしれないが，そう，健常高齢者における[^{11}C]PiB陽性者はまさにpreclinical AD患者とニアリーイコールと著者らは考えている．それでは，どれほどの患者数が存在するかというと，[^{11}C]PiB陽性者は健常高齢者の20-50％と著者らは見積もっている．高齢者を65歳以上とすると，我が国および先進国ではそれぞれ現時点で約3000万人および約2億人の65歳以上人口が存在し，またこれを基に算出されるpreclini-